Optimized autofluorescence bronchoscopy using additional backscattered red light

Tanja Gabrecht
Thomas Glanzmann
Swiss Federal Institute of Technology (EPFL)
Laboratory for Air and Soil Pollution
1015 Lausanne, Switzerland

Lutz Freitag
Clinic for Pneumology and Thoracic Surgery, Hemer
Pneumology Department
58675 Hemer, Germany

Bernd-Claus Weber
Richard Wolf Endoscopes GmbH
75438 Knittlingen, Germany

Hubert van den Bergh
Swiss Federal Institute of Technology (EPFL)
Laboratory for Air and Soil Pollution
1015 Lausanne, Switzerland

Georges Wagnières
Swiss Federal Institute of Technology (EPFL)
Institute of Chemical Sciences and Engineering
Photomedicine Group
1015 Lausanne, Switzerland

Abstract. Autofluorescence bronchoscopy (AFB) has been shown to be a highly sensitive tool for the detection of early endobronchial cancers. When excited with blue-violet light, early neoplasia in the bronchi tend to show a decrease of autofluorescence in the green region of the spectrum and a relatively smaller decrease in the red region of the spectrum. Superposing the green foreground image and the red background image creates the resultant autofluorescence image. Our aim was to investigate whether the addition of backscattered red light to the tissue autofluorescence signal could improve the contrast between healthy and diseased tissue. We have performed a clinical study involving 41 lung cancers using modified autofluorescence bronchoscopy systems. The lesions were examined sequentially with conventional violet autofluorescence excitation (430 nm ± 30 nm) and violet autofluorescence excitation plus backscattered red light (430 nm ± 40 nm plus 665 nm ± 15 nm). The contrast between (pre-)neoplastic and healthy tissue was quantified with off-line image analysis. We observed a 2.7 times higher contrast when backscattered red light was added to the violet excitation. In addition, the image quality was improved in terms of the signal-to-noise ratio (SNR) with this spectral design. © *2007 Society of Photo-Optical Instrumentation Engineers.*
[DOI: 10.1117/1.2811952]

1 Introduction

Carcinoma of the bronchi is the most common cancer and cause of cancer deaths in the world, with the highest incidence rates occurring in North America and Europe.[1–3] Bronchial cancer has a poor prognosis, mainly due to its progressive nature and because most cancers are detected at an advanced stage.[4] Prognosis is much more favorable if the cancer is detected and treated early, if possible at the *in situ* stage.[4–6] Bronchoscopy is the only established method that allows detection, localization, and definitive histological diagnosis of endobronchial lesions. Although the resolution of bronchoscopy is superior to that of chest radiography (CRX) and computed tomography (CT), conventional white light bronchoscopy (WLB) has important diagnostic limitations for detecting early cancerous and precancerous lesions. Sato et al.[7] have shown that for radiographically occult bronchial cancers in patients with positive sputum cytology, only about 30% of the lesions can be localized, with difficulty, by conventional bronchoscopy. It should be noted that the percentage of lesions missed during WLB is probably much larger, since numerous radiographically occult lesions were not detected during this study. This important clinical problem is central to the extensive research efforts performed by numerous groups to develop patient screening and cancer detection methods.[8,9] One promising approach to detect bronchial precancerous and early cancerous lesions during bronchoscopy is based on the imaging of the tissue autofluorescence.[8,10] While conventional WLB is based on the detection of minimal alterations in tissue surface structure, autofluorescence bronchoscopy (AFB) exploits the spectral and intensity contrast of the tissue autofluorescence existing between normal and pre-/early cancerous tissues.

AFB works by capitalizing on the decrease in tissue autofluorescence intensity within the green spectral region for pre- and early cancerous lesions as compared to healthy tissue under violet excitation.[8,11,12] This decrease can be visualized by specific endoscopic imaging devices.[13] In most cases, due to the three-dimensional (3-D) geometry of the bronchi, a second background image is obtained in the red part of the spectrum, to perform a contrast enhancement procedure between the contrast-bearing green and the non-contrast-bearing red images. Several endoscopic fluorescence imaging systems (Xillix LIFE system,[14] Storz D-Light system,[15] and Pentax 3000 system[16]) are based on this principle.

Numerous clinical studies have demonstrated that AFB used in addition to conventional WLB significantly increases

Address all correspondence to Georges Wagnières, Swiss Federal Institute of Technology (EPFL), Station 6, Building CH, 1015 Lausanne, Switzerland; Tel. +41 21 693 3120; Fax +41 21 693 3626; E-mail: georges.wagnieres@epfl.ch
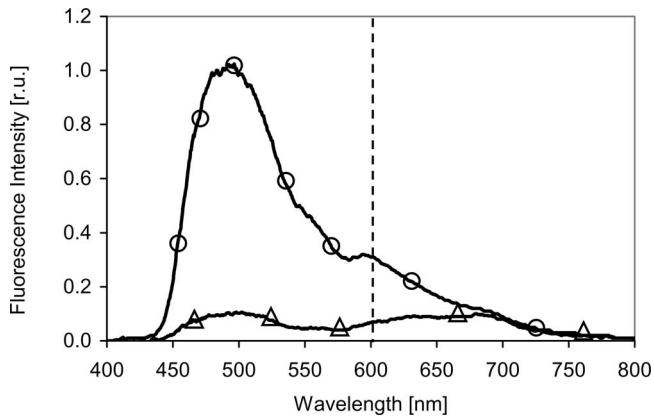
Fig. 1 Autofluorescence spectra from normal (circles) bronchial tissue and dysplasia/CIS (triangles) (adapted from Ref. 11). These spectra were obtained using an excitation of 405 nm, FWHM=10 nm with an optical fiber–based spectrofluorometer. The healthy tissue spectrum is dominated by a peak around 500 nm, i.e., in the green part of the spectrum, while the spectrum measured on dysplastic tissue shows equal intensities in the green and the red part of the visible spectrum. The dotted line separates the green, i.e., short-wavelength, region and the red, i.e., long-wavelength, region used to generate the foreground and background autofluorescence images, respectively.

the number of detected lesions,[8,10,14,17,18] increasing the sensitivity by a factor of 2. However, the higher sensitivity comes with a limited specificity.[8,19] Moreover, it should be noted that most of the AFB systems are likely to be suboptimal since their spectral designs are not based on the results of comprehensive studies of specific tissue autofluorescence properties. One exception is the system developed and produced by Richard Wolf GmbH. This system emerged from a systematic and comprehensive clinical study of the autofluorescence spectroscopy of normal tissues and precancerous and early cancerous lesions of the mucous membrane lining the tracheobronchial tree.[11,20] The group in Lausanne demonstrated that the highest contrasts between healthy and (pre-) malignant tissues are observed with excitation wavelengths around 405 nm. In addition, they observed that, at this excitation wavelength, a strong decrease of fluorescence intensity exists for these lesions in the green (below 590 nm) region of the spectrum, whereas this decrease is much smaller but still present in the red part of the spectrum (beyond 590 nm). Typical spectra from healthy and dysplastic bronchial mucosa excited at 405 nm are shown in Fig. 1. Since a small decrease is also observed in the red part of the AF spectrum, this group suggested a possible method to improve the performances of fluorescence bronchoscopy: using additional red backscattered light as a background instead of the red autofluorescence. According to Zellweger et al.,[11] using an optimized amount of red backscattered light should increase the contrast between healthy and pre-/early malignant tissue by a factor of 2. Moreover, the background image created by the backscattered red light enhances the brightness and consequently the quality of the endoscopic images. Last, the choice of backscattered red light appears to be a sensible spectral choice, as it is minimally influenced by changes of tissue properties, textures, and structures. It should be noted that a similar approach using backscattered red and near-infrared light was

reported by Zeng et al.[21] for autofluorescence imaging in the gastrointestinal tract.

The impact of these spectral improvements, according to our knowledge, has not previously been assessed quantitatively with imaging systems. Therefore, we have designed an endoscopic fluorescence imaging system that includes the features of violet excitation around 405 nm and offers the option to add red light to the excitation. This system was used for the clinical study reported here to confirm the results from Zellweger et al.[11] and to assess the potential of additional backscattered red light for improved contrast between healthy and (pre-)malignant tissue.

2 Materials and Methods

2.1 Instrumentation

We used a modified endoscopic fluorescence imaging (EFI) system developed in collaboration with the company Richard Wolf Endoskope GmbH, Knittlingen, Germany. The system consisted of a modified endoscopic light source, a filtered 3 CCD RGB camera (5137 Combilight PDD and EFI 5507 camera), and a dedicated bronchofibroscope. This experimental system offered the unique advantage of three different illumination/excitation modes that could be selected during the bronchoscopy using a simple foot switch. The light source contained an infrared (IR)-filtered 300-W Xe lamp and was equipped with a flip-flop filter holder allowing for change between white light illumination for conventional endoscopy and two different violet light excitations for autofluorescence endoscopy. The two violet fluorescence excitation filters used in our study were: a violet bandpass filter (pure violet: PV) with a transmission $\geq 95\%$ between 395 and 460 nm, and a double bandpass filter (violet plus red light: V+R) with a transmission $\geq 90\%$ between 390 to 470 nm and a second weak (8%) transmission between 650 nm to 680 nm. The transmission spectra of these filters are shown in Fig. 2. The slight spectral differences in the blue-violet bands were conditional of manufacturing but do not affect the excitation properties. Both filters transmit the same light energy, although the transmission band of the V+R filter is slightly broader than that of the PV filter. This is due to the lower transmission of the V+R filter relative to the PV filter. Both filters were used alternately during the endoscopic exams. The illumination/excitation light was transmitted from the light source to the endoscope via a liquid light guide (Type 4070.253, Richard Wolf GmbH, Knittlingen, Germany).

As can be seen in Fig. 3, the camera objective contained a 490-nm long-pass filter that was optimized to reject all violet excitation light. A communication cable connected the camera controller and the light source. When the light source was used in the conventional white light mode, the camera employed the standard video red, green, and blue color (RGB) mode. If the light source was used in one of the fluorescence excitation modes, the signal of the camera's blue channel was suppressed. Consequently, images taken in the fluorescence mode contained only the red and green image color information necessary to visualize the spectral contrast between healthy and precancerous tissue, as described in Sec. 1. The gamma factor of the camera-video unit was 0.71.

The camera head was clipped to a flexible bronchofibroscope. Unlike conventional bronchofibroscopes, this device
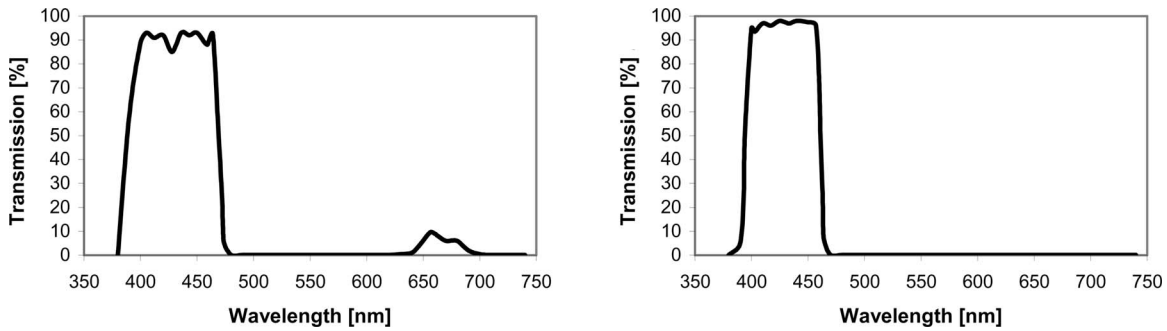
Fig. 2 Transmission spectra of the excitation filters. The transmission spectrum of the pure violet (PV) bandpass filter is shown on the left. The graph on the right shows the transmission characteristics of the double bandpass filter used for violet excitation in combination with the detection of the backscattered red light (V+R).

was equipped with illumination fiber bundles offering a high UV transmittance. The available total illumination power at the distal end of the bronchoscope was typically 120 mW with both excitation filters. This power was high enough to enable a real-time detection of the autofluorescence/reflectance images in the entire tracheo-bronchial tree at the video frequency. In addition, this camera enabled the user to perform a "dual" automatic white/color balance, as explained below. A block diagram of the system is shown in Fig. 3.

2.2 Study Design

A total of 41 patients were involved in this study, which was performed at the Center for Pneumology and Thoracic Surgery in Hemer, Germany.

The criteria for enrollment were: known or suspected carcinoma in the bronchi (standard diagnostic workup or pre-therapeutic bronchoscopy), and/or resection of lung cancer (follow-up bronchoscopy), and/or atypia in the sputum and/or abnormal x-ray findings as well as complaints of dyspnea or cough without suspect findings either in sputum or on x-ray.

Patients who had received photosensitizing agents like Photofrin, those known or suspected of suffering from pneumonia, and those considered generally unsuitable for bronchoscopy, such as patients with uncontrolled hypertension or bleeding disorders, were excluded from the study.

All the AFBs were performed according to the procedure approved by the local ethical committee of the Hemer Centre for Pneumology and Thoracic Surgery. All but three broncho-

scopies were carried out under local anaesthesia. The procedure was performed in two stages. First, conventional WLB was performed with the standard equipment used at the Hemer Center [Olympus endoscopic white light source with Olympus fiber optics (Type BF 40 and BF1T40) or Olympus video endoscope (BF 160)]. Then, the bronchoscope was changed in favor of the EFI system with its dedicated bronchofibroscope. Automatic white balancing (AWB) of the camera was always performed on a white cotton compress prior to endoscopy. Moreover, automatic color balancing (ACB) was performed for each autofluorescence excitation mode on the healthy main carina of the patient just after insertion of the bronchofibroscope. This ACB allowed us to correct for the interpatient fluctuations in the tissue autofluorescence intensity that were reported by Zellweger et al.[20]

Bronchoscopy was repeated first with the PV filter and then with the V+R filter. Tissue areas were classified as "suspicious" in the fluorescence mode when they exhibited a brownish or brown-reddish color with PV light excitation or a marked reddish color under V+R excitation, respectively.

All suspicious sites examined with the conventional WLB were then examined in the fluorescence mode and vice versa. Since the principal aim of our study was to access the effect of additional backscattered red light on the tumor/tissue contrast, and not to investigate the sensitivity and specificity of the system, no random biopsies were taken. However, the endobronchial position and visual aspect of all abnormal findings were noted. Biopsy specimens or brushes were obtained
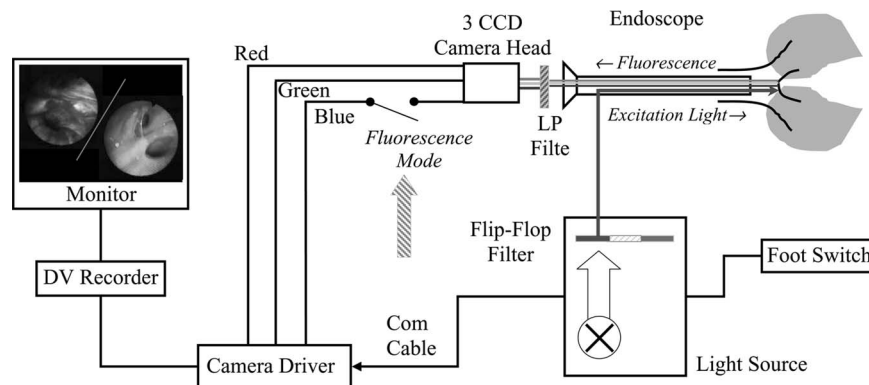

Fig. 3 Block diagram of the AF bronchoscopy system.

Table 1 Histological code and related histopathologies.

Category	Histology	Class	Group
1	Healthy	Normal	
2	Inflammation	Reactive changes	False positives
3	Metaplasia		
4	Mild dysplasia	(Pre-)neoplastic changes	True positives
5	Moderate dysplasia		
6	Severe dysplasia/CIS		
7	Epidermoid carcinoma		
8	Small cell carcinoma		
9	Adenocarcinoma		

from all sites suspicious either under WLB or AFB. Whenever possible, biopsies were taken under fluorescence examination to guarantee a precise uptake of the specimens even on small areas.

Biopsies were classified in a three-class-system with nine histologic categories: (1) normal tissue, (2) reactive changes, and (3) (pre-)neoplastic changes. Class 2 (reactive changes) included inflammation (code 2) as well as metaplasia (code 3). The class of (pre-)neoplastic changes (class 3) was subdivided into mild, moderate, and severe dysplasia/carcinoma *in situ* (CIS); squamous cell carcinoma, small cell carcinoma; and adenocarcinoma, corresponding to histologic categories 4 to 9, respectively. It should be noted that the tissue changes corresponding to categories 4 to 6 are considered preneoplastic lesions, whereas categories 7 to 9 are referred to as neoplasia.[22] Lesions classified as suspicious under fluorescence and attributed to classes 1 and 2 (categories 1 to 3) were referred to as fluorescence false positive results (FP), whereas those in class 3 (categories 4 to 9), were referred to as fluorescence true positive results (TP). Our histopathologic classification system is shown in Table 1.

2.3 Image Analysis

All EFI examinations were recorded in real time on a Sony digital video cassette recorder (Sony DSR-11, Sony, Japan). For analysis purposes, the video material was sifted. One image per biopsied area and examination mode (white light, pure violet excitation, and violet excitation plus additional red light) was digitized using the IEEE1394 interface of the videocassette recorder and a PCMCIA card (MovieCardBus, Aist MediaLab, Germany) in a portable computer. Digitization was in the 24-bit RGB color scheme.

Image analysis was performed to quantify the red and green intensity ratios between lesions and the surrounding healthy tissue. The average intensity of the red and green pixels of the biopsied site (lesion), of a healthy tissue site next

to the lesion (control), and of the surrounding presumably healthy tissue (reference) were computed with their standard deviations. All computed values were corrected for the gamma function of the camera system.

The red and green intensity of a biopsied area was then divided respectively by the red and green intensities obtained from the surrounding healthy tissue in order to correct the recorded intensities for interpatient fluctuations and the color balance of the camera. The corresponding ratios for the healthy tissue areas were computed in the same way. We computed the mean values and standard deviations for each histopathologic class.

Descriptive statistics were used to summarize the detection of the TPs and FPs with the two excitation modes using the Student's t-test. Comparison between the groups was performed based on the confidence interval (CI) and the single-sided p-value (p). A confidence interval of 95% and a p-value $p < 0.05$ were considered significant.

Sensitivity-specificity analysis was performed using receiver operating characteristics (ROC) analysis, assuming normal distributions of the normalized ratios. The performances of the two autofluorescence methods (PV and V+R) were compared as described by Metz:[23] the false positive fractions (FPF) obtained with the PV and the V+R detection were compared for a given true positive fraction (TPF).

3 Results

3.1 Patients and Histopathology Breakdown

Among the 41 patients included in the study, a total of 27 patients had at least one suspicious site (in the following called a "positive case"), whereas 14 patients showed no suspect bronchoscopic findings during conventional WLB or AFB. In four cases of pretherapeutic bronchoscopy, the histopathology of the observed lesions was known from former examinations (the delay between the first WLB and the subsequent AFB was less than 8 weeks). In all other patients, a biopsy was taken from each suspect site, resulting in a total of 36 specimens.

The histopathologic diagnoses for these 40 positive cases were as follows: 15 normal tissue, 8 inflammation and metaplasia, and 17 (pre-)neoplastic changes (9 squamous cell carcinoma, 2 mild dysplasia, 1 moderate dysplasia, 3 severe dysplasia, 1 adenocarcinoma, and 1 small cell carcinoma).

In 23 of these positive cases, a direct comparison of PV excitation and V+R excitation AFB was performed on the same bronchial site. In 3 positive cases, only images recorded under pure violet light excitation were available, whereas in the remaining 14 positive cases, only violet excitation plus backscattered red light could be applied. Since more positive cases were examined with the V+R filter than with the PV filter, we will refer only to positive cases examined with the V+R filter to discuss the visibility of AFB and conventional WLB.

3.2 Assessment of the Positive Predictive Value (PPV) of AFB and WLB

All positive cases were, by definition, visible either with AFB and/or with conventional WLB. Whenever AFB was performed with the PV and the V+R filter in the same patient, tissue sites looking suspicious with the PV filter excitation

Table 2 Visibility of positive cases examined with WL and by AFB. Visibility of the biopsied sites considered suspicious under conventional white light illumination and/or with the V+R autofluorescence excitation according to their histopathology. Visibility of the lesions using WLB or AFB are labeled W+ and F+, respectively. Cases invisible under WLB and AFB are labelled W− and F−, respectively.

Category		F+ and W+	F+ and W−	F− and W+
		AFB:FP;WL:FP	AFB:FP;WL:TN	AFB:TN;WL:FP
1	Healthy	10	3	1
2	Inflammation	2	2	1
3	Metaplasia	2	0	0
		AFB:TP;WL:TP	AFB:TP;WL:FN	AFB:FN;WL:TP
4	Mild dysplasia	1	1	0
5	Moderate dysplasia	1	0	0
6	Severe dysplasia/CIS	2	1	0
7	Squamous cell Carcinoma	6	2	0
8	Small cell Carcinoma	1	0	0
9	Adeno Carcinoma	1	0	0

were also suspicious with the V+R filter, and vice versa. However, the fluorescence contrast between the suspect site and the surrounding healthy tissue was always better with the V+R filter. Table 2 shows the visibility of the 37 positive cases examined with the V+R filter according to their histopathologic status. These cases include 16 histopathologic positive lesions (i.e., categories 4 to 9) and 21 histopathologic negative lesions (i.e., categories 1 to 3). Suspect sites as determined under WL examination were classified as white light positive (W+), and those determined with the AF excitation were classified as fluorescence positive (F+). Unsuspicious sites in WLB and AFB were labeled white light negative (W−) and fluorescence negative (F−), respectively. All 16 malignant lesions examined with AFB exhibited positive fluorescence. Among them, 12 (75%) were also visible under white light examination, and consequently, 4 (25%) of the malignant lesions were occult with conventional WLB. In addition, no lesion was visible during WLB and negative under fluorescence. Twenty-one (57%) of all cases showed no abnormalities in histopathology apart from inflammation and metaplasia and were therefore considered as bronchoscopical false positives (FP). Nineteen (90%) of these FP cases showed positive fluorescence, and 16 (76%) of the FP cases were considered suspicious during WL examination. Two of these latter 16 FP cases were incorrectly classified as suspicious by white light endoscopy only but were not suspicious under fluorescence. Five of the bronchoscopical false positive cases were suspect under fluorescence only but not under white light. Theses results are summarized in Table 3. These results suggest that the sensitivity of AFB is better than that of WLB.

3.3 Illustrations of WLB and AFB Imaging

The following images show true positive lesions examined with WLB, PV fluorescence excitation, and V+R fluorescence excitation.

Figure 4 shows a mild dysplasia presented by a 62-year-old male patient observed with conventional WLB and AFB with PV and V+R fluorescence excitation, respectively. This patient was known to suffer from a squamous cell carcinoma in the upper right bronchus and underwent pretherapeutic bronchoscopy for treatment by photodynamic therapy. The images show the division between the middle and lower lobe. The spur was slightly suspicious with WLB due to thickening and reddening.

AFB exhibited a sprawled brownish area on the olive-green healthy tissue background under pure violet excitation. The same area is clearly visible as a bright red zone on a clear green background when backscattered red light is used in addition to the violet excitation.

These images illustrate the improved detectability and demarcation of the extension of superficial bronchial lesions if AFB is used instead of WLB. Moreover, the use of the V+R excitation filter clearly allows us to generate much better images than the PV filter. In addition, the images obtained with the V+R excitation are much brighter and less noisy than their counterparts obtained with PV excitation only. This is due to an enhancement of the chromatic contrast between the lesion and the surrounding healthy tissue.

Table 3 Number of true positive (TP) and false positive (FP) as well as the true negative (TN) and false negative (FN) cases for WLB and AFB with backscattered red light.

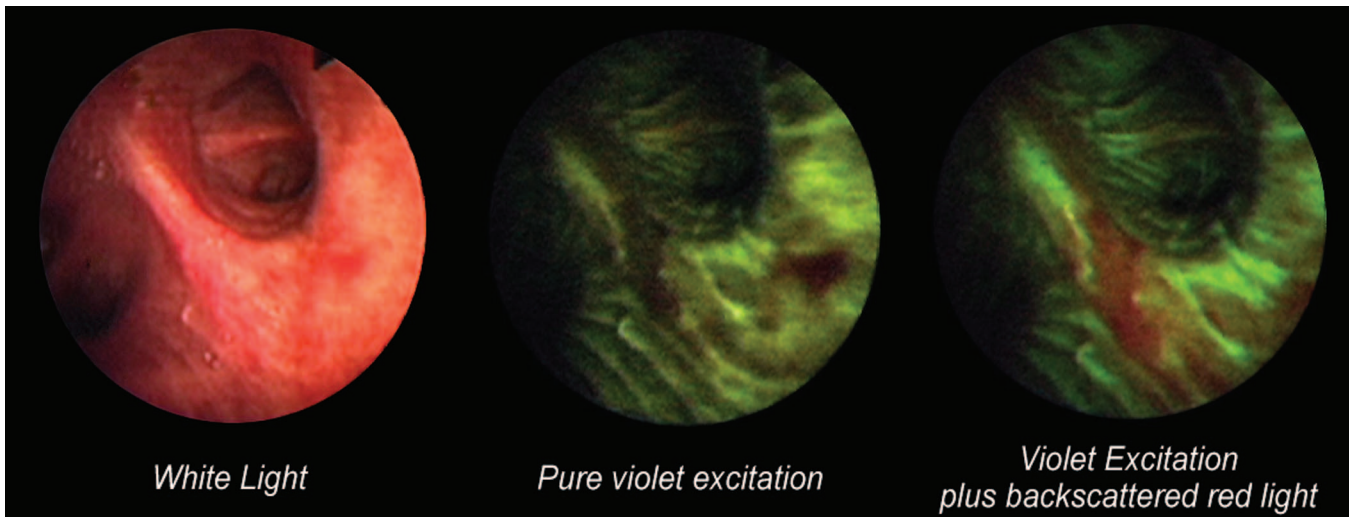|	TP	FN	FP	TN
AFB	16	0	19	2
WL	12	4	16	5

Fig. 4 Mild dysplasia. The lesion on the spur is hardly suspicious with WLB but appears as a sprawled brownish area with AFB using pure violet excitation light. When violet excitation plus additional backscattered red light is used, the lesion appears as a marked reddish area on the greenish surrounding tissue. Moreover 3-D perception is enhanced in the latter image.

Figure 5 illustrates the effect of backscattered red light on the background image in the red color channel. The AF images from a case of severe dysplasia observed with PV and V+R excitation were separated into their green (left image) and red (right image) channels, respectively, and are presented in gray scale. The lesion is visible as a dark, sharp circumscribed area on the base of the spur. In the case of PV excitatio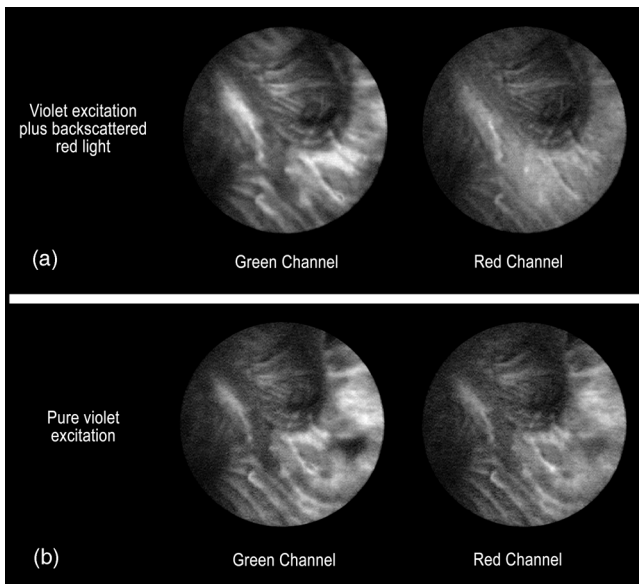n [Fig. 5(a)], both the green and the red channel images show an intensity decrease on the site of the lesion. In the case of V+R excitation [Fig. 5(b)], the red channel image exhibits a nearly homogenous intensity distribution, while the green channel image shows an intensity decrease on the site of the lesion. It should be noted that the spur was not classified as suspicious during WLB.

3.4 Image Analysis

The mean normalized red-to-green ratios computed from image analysis of fluorescence positive areas and the fluorescence negative healthy reference zones are shown in Fig. 6 for both fluorescence excitation modes. Their values and standard deviations are shown for the different histopathologic classes—normal tissue (squares), reactive changes (triangles), and (pre-)neoplastic changes (diamonds). The circles depict the mean ratios from the fluorescence negative healthy reference zones.

In the case of pure violet excitation, the mean ratios were comparable for false positive normal ($\text{mean}_{normal} = 1.66 \pm 0.39$), reactive ($\text{mean}_{reactive} = 1.75 \pm 0.12$), and (pre-)neoplastic changes ($\text{mean}_{(pre-)neoplastic} = 1.74 \pm 0.43$). It should be noted that the mean value of the normalized ratio for the fluorescence-negative healthy reference zone was $\text{mean}_{reference} = 1.03 \pm 0.05$. Adding backscattered red light to the violet excitation increased the corresponding mean values by a factor of about 2 for the normal and reactive changes classes ($\text{mean}_{normal} = 3.65 \pm 0.43$, $\text{mean}_{reactive} = 4.04 \pm 0.48$). For the (pre-) malignant lesions, this factor exceeded the value of 2.7 ($\text{mean}_{(pre-)neoplastic}$ for violet plus red $= 4.93 \pm 2.25$). The mean value of the normalized ratio for the fluorescence-negative healthy reference zone remained in the range of 1 ($\text{mean}_{reference} = 1.10 \pm 0.16$).

The signal-to-noise ratio (SNR), defined as the average pixel intensity of the analyzed tissue sites divided by its standard deviation, was by a factor of about 2 higher for the V+R excitation (SNR=8.8) than for the pure violet excitation (SNR=4.5).

Fig. 5 Influence of the backscattered red light on the image background. These images present the same lesion as in Fig. 4, but with the fluorescence images split into their green and red color channels. They are presented in grayscale mode. Addition of backscattered red light to the violet fluorescence excitation light (a) results in a nearly homogenous background in the red channel image. The corresponding image obtained with PV excitation (b) shows demarcated zones of decreased intensity, influencing the contrast between diseased and healthy tissue areas.
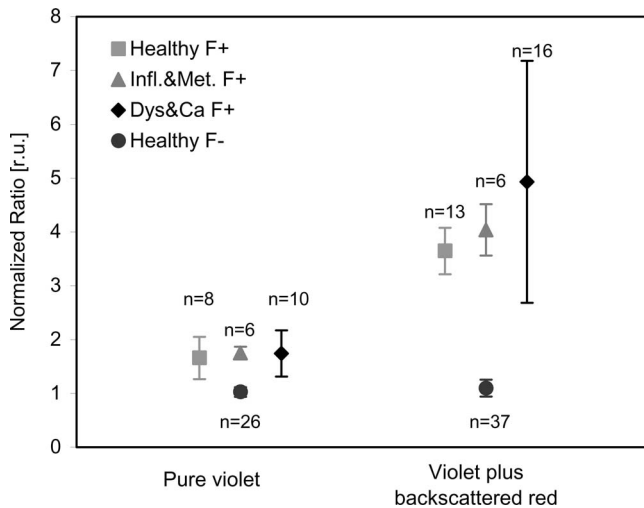
Fig. 6 Mean values of normalized ratios for both pure violet and violet+red excitation. This graphic depicts the mean values of the normalized ratios for pure violet excitation (data on the left) and violet excitation with backscattered red light (data on the right). Circles denote values for healthy and fluorescence-negative tissue, squares denote healthy but fluorescence-positive tissue, triangles denote reactive changes (inflammation and metaplasia), and diamonds denote (pre-)neoplastic changes (dysplasia and carcinoma). The number of cases, n, is given for each histopathologic class.

The ROC comparative analysis was based on a TPF of 0.66 (66%). The corresponding FPFs for the PV method were 0.61 (fluorescence positive FP, but healthy) and 0.95 (reactive tissue changes). The corresponding values for the V+R method were 0.26 (healthy) and 0.6 (reactive changes).

4 Discussion

AFB has proven to be an efficient and useful tool in the detection of premalignant lesions and early cancers in the bronchi. In this study, we present an optimized AFB imaging system offering superior color contrast between healthy tissue and lesions.

One of the major problems encountered by most commercially available AFB systems is the poor image quality. This is due to the limited tissue autofluorescence intensity, combined with the limited light collection efficiency, throughput, and physical sensitivity of the imaging system.[24] Our system employed a filtered Xe-lamp light source in combination with a fibroscope specially designed for autofluorescence detection with an excitation wavelength around 405 nm. Used in combination with a 3 CCD endoscopic color camera, we obtained noise-reduced fluorescence images at video frequency, i.e., about 25 frames per second for PAL video, bright enough for a proper navigation in the tracheo-bronchial tree. This enabled the physician to perform the entire bronchoscopy in the autofluorescence mode instead of examining the bronchial tree in the conventional white light mode, switching to the autofluorescence mode only at specific sites.

Due to the 3-D geometry of the organ, autofluoresence detection in the bronchi requires the detection of both a background and a contrast-bearing foreground image. Such a background image can be created by backscattered light detected in one or several different color channels.

Profio[25] and Leonhard[15] reported the detection of a small amount of backscattered blue excitation light to optimize the quality of autofluorescence detection in the bronchi. Indeed, the use of blue/violet backscattered light helps to reveal the texture of the bronchi, but it is not ideal for correcting the autofluorescence images detected in the green spectral domain. Consequently, following the spectrofluorometric study of the bronchial autofluorescence performed by our group,[11] we investigated the use of backscattered red light for the optimization of our imaging system.

We demonstrated in the study presented in this paper that the combination of violet light induced tissue autofluorescence with backscattered red light increases the red-to-green color ratios between normal and (pre-)neoplastic tissue areas in the AFB images by a factor of about 2.7 compared to violet-light-induced fluorescence alone. This factor corresponds to the autofluorescence intensity ratio measured spectroscopically in the red part of the spectrum, i.e., between 600 and 800 nm, between healthy and malignant tissues reported by Zellweger et al.[11] This twofold to threefold increase of the red-to-green ratio is responsible for the improved chromatic contrast perceived in the V+R fluorescence images. Indeed, the bright red appearance of fluorescence positive lesions excited with violet light and backscattered red light are more easily perceived on the green background characteristic of healthy tissue than the brownish-olive colored lesions observed under pure violet excitation. Moreover, the red background image created by the backscattered red light dramatically improves the SNR, allowing better navigation and orientation for the endoscopist in the autofluorescence mode. In addition, the use of the V+R excitation filter strongly suggests an increase in specificity, as indicated by Fig. 6. The overlap between the distribution of the normalized ratio measured in true positive and false positive sites is much smaller with the V+P filter than with the PV filter, indicating a more pronounced demarcation. This is confirmed by the results from the ROC analysis, which showed that for a TPF of 0.66, the corresponding FPF was lower by a factor of about 2 for the V+R excitation than for the PV excitation.

Normal, reactive changes and (pre-)neoplastic fluorescence positive sites showed no significant differences in their normalized red-to-green ratios under PV excitation (CI 95%, $p > 0.283$). When additional backscattered red light was used, a significant difference could be observed between fluorescence positive but histopathologically normal sites (false positives, FP) and fluorescence positive (pre-)neoplasia (true positives, TP) (CI 95%, $p = 0.023$). A much weaker difference (CI 80%, $p = 0.098$) was observed between the ratios computed from the FP reactive changes and the TP (pre-)neoplasia excited with the V+R excitation.

The ratios computed from the healthy fluorescence negative controls were all significantly different (CI 95%) than the ratios computed from the fluorescence true positive (pre-)neoplastic and the false positive healthy or reactive sites for both the PV and V+R filter. However, the p-values computed for the fluorescence negative controls and the fluorescence positive normal, reactive changes and (pre-)neoplastic lesions were by one to seven orders of magnitude lower for the V+R excitation [normal $p = 4.21 \times 10^{-4}$, reactive changes $p = 1.24 \times 10^{-5}$, and (pre-)neoplasia $p = 2.99 \times 10^{-6}$] than for the PV excitation (normal $p = 1.31 \times 10^{-3}$, reactive changes

$p = 1.45 \times 10^{-5}$, and (pre-)neoplasia $p = 2.79 \times 10^{-4}$). Moreover, it is worth noting that the SNR improved by a factor of about 2 when V+R excitation was used. Therefore, the results presented in this paper indicate that the addition of backscattered red light provides an opportunity to better discriminate lesions and healthy tissue. We would like to emphasize that the results obtained in this study do not allow us to compute the sensitivity or specificity of AFB, since no random biopsies were taken.

The issue of false positive tissue sites has already been reported by other authors using commercial systems based on violet autofluorescence excitation.[26–29] Several reasons may account for the high number of false positives. It is likely that some type of somehow atypical but noncancerous tissues appear positive under AFB, including scar tissue,[28] inflammation, and bruised mucosa. Therefore, the patient inclusion criteria of our study (patients with known endobronchial lesions, lung cancer follow-up patients, or high-risk patients suspect for endobronchial lesions) can influence the false positive rates. In the study presented here, about 45% of all patients exhibiting fluorescence positive sites correspond to the latter two groups. Clinical studies including these types of patient groups frequently report increased false positive rates.[30–32] Another source of false positives in clinical studies is related to the procedure of taking a biopsy. Whenever possible, biopsies were taken under fluorescence light excitation to assure that the tissue sample was taken from the fluorescence positive area. Nevertheless, it cannot be excluded that a certain number of tissue samples were not taken from the fluorescence positive regions, but from neighboring nonfluorescent tissue. Last, histopathologic examination is deemed as the "gold standard" for comparison with bronchoscopic findings in nearly all clinical studies reporting on autofluorescence bronchoscopy. Nevertheless, some authors report on significant interobserver variability in histopathologic reporting.[33,34] In a retrospective study of 343 bronchial tissue samples from AFB, Venmans et al.[34] revealed interobserver variability by a factor of 2 in the number of diagnosed preinvasive bronchial neoplasias. Thus, the interobserver variability in the histologic analysis of preinvasive bronchial tissue changes has an influence on the results of conventional bronchoscopy as well as AFB. The tissue samples obtained in our study were analyzed on a single-view basis only, i.e., each biopsy was analyzed by a single pathologist. It is therefore very likely that a certain number of AFB positive but histologically reported negative, i.e., AFB false positive cases, are in reality AFB true positive results. This would dramatically change the values of sensitivity and PPV. Independent revision of the samples by two or more histopathologists might reduce such errors. The distribution of the normalized ratio for the healthy tissue is of particular interest in this context. Indeed, this distribution seems to be bimodal, the true negative sites being closely grouped around the value of one, whereas the normalized ratios of the false positive site are grouped at much larger values. This effect is particularly visible with the V+R excitation. It should be noted that the two sources of possible incorrect histopathologic assignations, i.e., the precision of tissue sampling and the interobserver variability, could explain the bimodal distribution of the ratios corresponding to the healthy tissues.

Large interpatient fluctuations of the normalized red-to-green ratios within the histologic classes were observed with both excitation modes. These fluctuations were more marked when backscattered red light was added to the violet excitation. This is indeed a drawback of the method. Analysis of the origins of these variations will lead to a better understanding of this phenomenon. Interpatient fluctuations in the AF were reported from several spectrofluorometric studies in the bronchi[20] and in other organs.[21,35] Since an important contribution to the fluctuations of the tissue autofluorescence intensity can be attributed to the inter- and intrapatient variations in fluorochrome concentrations and epithelium thickness, these fluctuations are more or less proportional in the green and red parts of the spectrum (intrinsic fluctuations).[11,20,36] However, this proportionality is no longer present if red backscattered light is detected instead of red autofluorescence. It should be noted that a similar phenomenon is present regarding the intensity of the excitation light available for the excitation of the fluorochromes. Indeed, our fluorescence imaging system uses an excitation band around 410 nm, corresponding to one absorption peak of hemoglobin. The main alterations in the local intensity of violet light available for excitation of the tissue autofluorescence are therefore related to the presence and extent of blood and blood-containing structures, i.e., for instance, the density, size, and depth of the blood vessels underlying the bronchial epithelium. These factors can vary markedly from one site to another. In the case of pure violet excitation, both the green and the red autofluorescence images are detected. A decrease in the violet excitation light due to the abovementioned local blood-containing structures therefore results in a nearly proportional decrease in the green as well as in the red part of the spectrum. Consequently, in the case of pure violet excitation, the inter- and intrapatient variations of the red-to-green ratios are minimally influenced by the blood-related fluctuations of the excitation light intensity. When backscattered red light is used in addition to the violet excitation, only the autofluorescence in the green image will be influenced by the absorption of the excitation light.

The enhanced chromatic contrast between a lesion and its healthy surrounding tissue allows a precise demarcation of the lesion's margins. This makes AFB an important tool, not only for diagnostic but also for pretherapeutic and presurgical bronchoscopy, where the determination of tumor margins is crucial for the planning and outcome of the treatment or surgery.

In summary, the results presented in this paper demonstrate that the additional detection of backscattered red light in violet-light-induced AFB has the potential to significantly increase the chromatic contrast between healthy and abnormal bronchial tissues. Moreover, the additional light markedly reduces the SNR, thus improving the image quality. This is of high interest for the development of future AFB systems. In the study presented here, each bronchoscopy was performed with fiber optic endoscopes equipped with an endoscopic camera clipped to the endoscope's eyepiece. However, the use of flexible videobronchoscopes has increased dramatically in recent years. It should be noted that autofluoresence videobronchoscopy systems have been commercially available for several years. The implementation of the principle of V+R detection has the potential to further improve the image quality and healthy-to-lesion contrast in those systems.

References

1. A. Jemal, T. Murray, A. Ghafoor, A. Samuels, E. Ward, M. J. Thun, R. C. Tiwari, and E. J. Feuer, "Cancer Statistics, 2004," *Ca-Cancer J. Clin.* **54**(1), 8–29 (2004).
2. F. Levi, F. Lucchini, C. La Vecchia, E. Negri, and F. Levi, "Trends in mortality from major cancers in the European Union, including acceding countries, in 2004," *Cancer* **101**(1), 2843–2850 (2004).
3. J. E. Tyczynski, F. Bray, and D. M. Parkin, "Lung cancer in Europe in 2000: epidemiology, prevention, and early detection," *Lancet Oncology* **4**(1), 45–55 (2003).
4. A. Jemal, L. X. Clegg, E. Ward, L. A. G. Ries, X. Wu, P. M. Jamison, P. A. Wingo, H. L. Howe, R. N. Anderson, and B. K. Edwards, "Annual report to the nation on the status of cancer, 1975–2001, with a special feature regarding survival," *Cancer* **101**(1), 3–27 (2004).
5. H. Kato, "Photodynamic therapy for lung cancer—a review of 19 years' experience," *J. Photochem. Photobiol., B* **42**(2), 96–99 (1998).
6. G. Bepler, B. Djulbegovic, R. A. Clark, and M. Tockman, "A systemic review and lessons learned from early lung cancer detection trial using low-dose computed tomography of the chest," *Cancer Control* **10**(4), 306–324 (2003).
7. M. Sato, Y. Saito, K. Usuda, S. Takahashi, M. Sagawa, and S. Fujimura, "Occult lung cancer beyond bronchoscopic visibility in sputum-cytology positive patients," *Lung Cancer* **20**(1), 17–24 (1998).
8. G. Wagnières, A. McWilliams, and S. Lam, "Lung cancer imaging with fluorescence endoscopy," in *Handbook of Biomedical Fluorescence*, M.-A. Myceck and B. W. Pogue, Eds., pp. 361–396, Marcel Dekker, Inc., New York (2003).
9. K. Shibuya, H. Hoshino, M. Chiyo, K. Yasufuku, T. Iizasa, Y. Saitoh, M. Baba, K. Hiroshima, H. Ohwada, and T. Fujisawa, "Subepithelial vascular patterns in bronchial dysplasias using a high magnification bronchovideoscope," *Thorax* **57**(10), 902–907 (2002).
10. D. Goujon, M. Zellweger, A. Radu, P. Grosjean, B.-C. Weber, H. van den Bergh, P. Monnier, and G. Wagnières, "*In vivo* autofluorescence imaging of early cancers in the human tracheobronchial tree with a spectrally optimized system," *J. Biomed. Opt.* **8**(1), 17–25 (2003).
11. M. Zellweger, P. Grosjean, D. Goujon, P. Monnier, H. van den Bergh, and G. Wagnières, "*In vivo* autofluorescence spectroscopy of human bronchial tissue to optimize the detection and imaging of early cancers", *J. Biomed. Opt.* **6**(1), 41–51 (2001).
12. J. Hung, S. Lam, J. LeRiche, and B. Palcic, "Autofluorescence of normal and malignant bronchial tissue," *Lasers Surg. Med.* **11**(2), 99–105 (1991).
13. G. Wagnieres, W. Star, and B. Wilson, "*In vivo* fluorescence spectroscopy and imaging for oncological applications," *Photochem. Photobiol.* **68**(5), 603–632 (1998).
14. S. Lam, T. Kennedy, and M. Unger, "Localization of bronchial intraepithelial neoplastic lesions by fluorescence bronchoscopy," *Chest* **113**(3), 696–702 (1998).
15. M. Leonhard, "New incoherent autofluorescence/fluorescence system for early detection of lung cancer," *Diagnostic Therapeutic Endosc.* **5**(2), 71–75 (1999).
16. N. Ikeda, H. Honda, A. Hayashi, J. Usuda, Y. Kato, M. Tsuboi, T. Ohira, T. Hirano, H. Kato, H. Serizawa, and Y. Aoki, "Early detection of bronchial lesions using newly developed videoendoscopy-based autofluorescence bronchoscopy," *Lung Cancer* **52**(1), 21–27 (2006).
17. P. Pierard, B. Martin, J.-M. Verdebout, J. Faber, M. Richez, J.-P. Sculier, and V. Ninane, "Fluorescence bronchoscopy in high-risk patients—a comparison of LIFE and Pentay systems," *J. Bronchol.* **8**(4), 254–259 (2001).
18. T. G. Sutedja, H. Condrigton, E. K. Risse, R. H. Breuer, J. C. van Mourik, R. P. Golding, and P. E. Postmus, "Autofluorescence bronchoscopy improves staging of radiographically occult lung cancer and has an impact on therapeutic strategy," *Chest* **120**(4), 1327–1332 (2001).
19. F. R. Hirsch, S. A. Prindiville, Y. E. Miller, W. A. Franklin, E. C. Dempsey, J. R. Murphy, P. A. Bunn, Jr., and T. C. Kennedy, "Fluorescence versus white-light bronchoscopy for detection of preneoplasic lesions: a randomized study," *J. Natl. Cancer Inst.* **93**(18), 1385–1391 (2001).
20. M. Zellweger, D. Goujon, R. Conde, M. Forrer, H. van den Bergh, and G. Wagnières, "Absolute autofluorescence spectra of human healthy, metaplastic, and early cancerous bronchial tissue *in vivo*", *Appl. Opt.* **40**(22), 3784–3791 (2001).
21. H. Zeng, A. Weiss, R. Cline, and C. E. MacAulay, "Real-time endoscopic fluorescence imaging for early cancer detection in the gastrointestinal tract," *Bioimaging* **6**(4), 151–165 (1998).
22. E. D. Travis, T. V. Colby, B. Corrin, Y. Shimosato, and E. Brambilla, in collaboration with L. H. Sobin and pathologists from 14 countries, *World Health Organization International Histological Classification of Tumours. Histological Typing of Lung and Pleural Tumours*, Springer Verlag, Berlin (1999).
23. C. E. Metz, "Basic principles of ROC analysis," *Semin Nucl. Med.* **8**(4), 283–298 (1978).
24. G. Wagnières, A. P. Studzinski, D. R. Braichotte, P. Monnier, C. Depeursinge, A. Châtelain, and H. Van Den Bergh, "Clinical imaging fluorescence apparatus for the endoscopic photodetection of early cancers by use of Photofrin II," *Appl. Opt.* **36**(22), 5608–5620 (1997).
25. A. E. Profio, D. R. Doiron, and J. Sarnaik, "Fluorometer for endoscopic diagnosis of tumors," *Med. Phys.* **11**(4), 516–520 (1984).
26. N. Ikeda, H. Honda, T. Katsumi, T. Okunaka, K. Furukawa, T. Tsuchida, K. Tanaka, T. Onoda, T. Hirano, M. Saito, N. Kawate, C. Konaka, H. Kato, and Y. Ebihara, "Early detection of bronchial lesions using lung imaging fluorescence endoscope," *Diagnostic Therapeutic Endosc.* **5**(2), 85–90 (1999).
27. M. Kakihana, K. Kyong II, T. Okunaka, K. Furukawa, T. Hirano, C. Konaka, H. Kato, and Y. Ebihara, "Early detection of bronchial lesions using system of autofluorescence endoscopy (SAFE) 1000," *Diagnostic Therapeutic Endosc.* **5**(2), 99–104 (1999).
28. K. Häußinger, F. Stanzel, R. M. Huber, J. Pichler, and S. H. Stepp, "Autofluorescence detection of bronchial tumors with the D-Light/AF," *Diagnostic Therapeutic Endosc.* **5**(2), 105–112 (1999).
29. T. Horvath, M. Horvathova, F. Salajka, B. Habanec, L. Foretova, J. Kana, H. Koukalova, P. Pafko, F. Wurst, E. Novotna, J. Pecina, V. Vagunda, R. Vrbacky, R. Talac, H. Coupkova, and Z. Pacovsky, "Detection of bronchial neoplasia in uranium miners by autofluorescence endoscopy (SAFE-1000)," *Diagnostic Therapeutic Endosc.* **5**(2), 91–98 (1999).
30. P. Vermylen, P. Pierard, C. Roufosse, T. Bosschaerts, A. Verhest, J. P. Sculier, and V. Ninane, "Detection of bronchial preneoplastic lesions and early lung cancer with fluorescence bronchoscopy: a study about its ambulatory feasibility under local anaesthesis," *Lung Cancer* **25**(3), 161–168 (1999).
31. B. J. W. Venmans, T. J. M. van Boxem, E. T. F. Smit, P. E. Postmus, and T. G. Sutedja, "Results of two years experience with fluorescence bronchoscopy in detection of preinvasive bronchial neoplasia," *Diagnostic Therapeutic Endosc.* **5**, 77–84 (1999).
32. S. Lam, C. MacAulay, J. C. leRiche, and B. Palcic, "Detection and localization of early lung cancer by fluorescence bronchoscopy," *Cancer* **89**(S11), 2468–2473 (2000).
33. J. M. Kurie, J. S. Lee, R. C. Morice, L. W. Garrett, F. R. Khuri, A. Broxson, Y. R. Jae, A. F. Wilbur, Y. Ren, and K. W. Hong, "Autofluorescence bronchoscopy in the detection of squamous metaplasia and dysplasia in current and former smokers," *J. Natl. Cancer Inst.* **90**(13), 991–995 (1998).
34. B. J. Venmans, H. C. van der Linden, H. R. Elbers, T. J. van Boxem, E. F. Smit, R. E. Postmus, and T. G. Sutedja, "Observer variability in histopathologic reporting of bronchial biopsy specimens—influence on the results of autofluorescence bronchoscopy in detection of preinvasive bronchial neoplasia," *J. Bronchol.* **7**(3), 210–214 (2000).
35. N. Ramanujam, M. F. Mitchell, A. Mahadevan, S. Thomsen, A. Malpica, T. Wright, N. Atkinson, and R. Richards-Kortum, "Spectroscopic diagnosis of cervical intraepithelial neoplasia (CIN) *in vivo* using laser-induced fluorescence spectra at multiple excitation wavelengths," *Lasers Surg. Med.* **19**(1), 63–74 (1996).
36. R. Richards-Kortum and E. Sevick-Muraca, "Quantitative optical spectroscopy for tissue diagnosis," *Annu. Rev. Phys. Chem.* **47**(1), 555–606 (1996).